Supporting information for:

Mechanistic Insights into the Crystallization of

Amorphous Calcium Carbonate (ACC)

Table S1 Summary of experimental conditions. SI is saturation index with respect to vaterite.

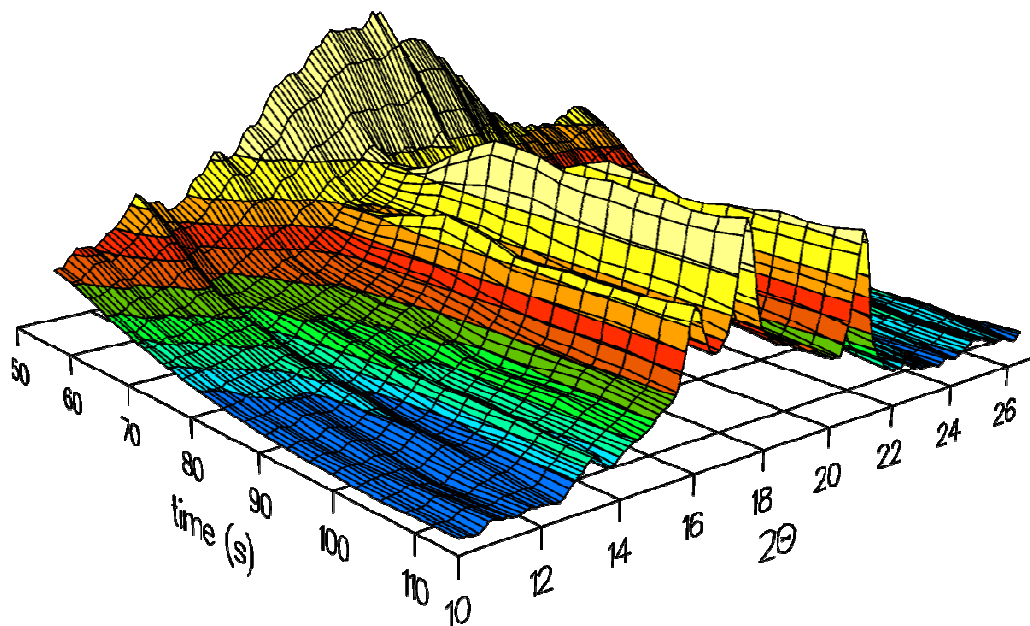|	$CaCl_2$ solutions		Na_2CO_3/Na_2SO_4 solutions			Solutions after mixing and prior to precipitation				
Experiment	Ca (M)	Volume (ml)	CO_3 (M)	SO_4 (M)	Volume (ml)	Ca (M)	CO_3 (M)	SO_4 (M)	Volume (ml)	SI
Pure ACC	1	100	1	-	100	0.5	0.5	-	200	4.2
$SO_{4(repl)}$	1	100	0.9	0.1	100	0.5	0.45	0.05	200	4.2
$SO_{4(add)}$	2.5	40	0.625	0.0625	160	0.5	0.5	0.05	200	4.2

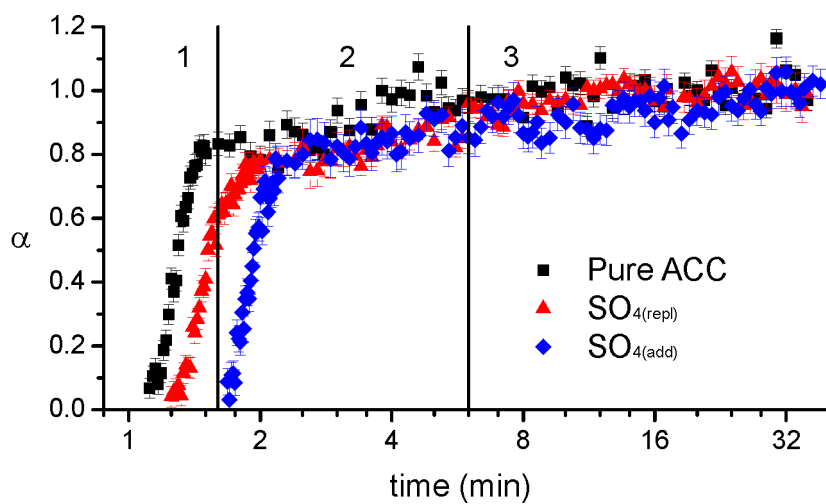Figure S1 3D representations of the time resolved WAXS patterns from first 2 minutes of the pure ACC experiment.

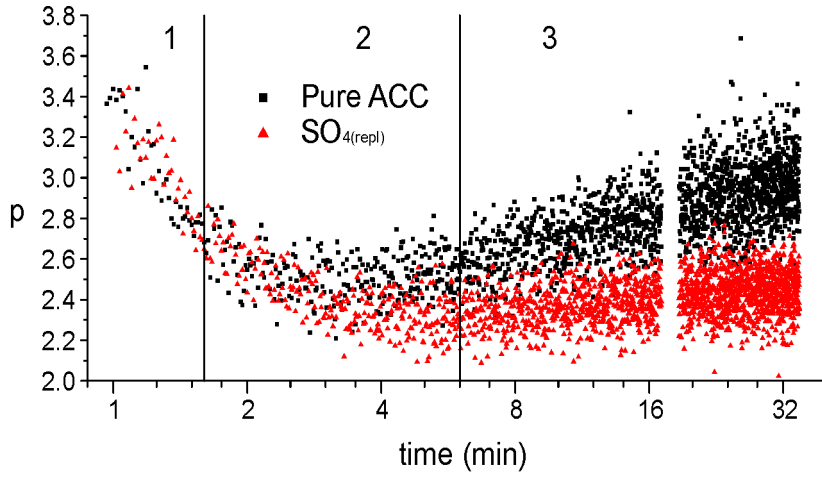Figure S2 $\alpha_{vaterite}$ plots for the pure ACC, $SO_{4(add)}$ and $SO_{4(repl)}$ experiment; time is plotted on a base 2 log scale.

Figure S3 The slope of the Porod region ($I(q) \propto q^{-p}$) calculated from the SAXS patterns for the pure ACC and SO$_{4(repl)}$ experiments as a function of time (on a base 2 log scale)

The value of the slope (p) of the Porod region (high q values in SAXS data; Figure S3) can give information on the fractal dimensions of scattering particles and surfaces.[1-3] Figure S3 shows that in the first ~4 minutes of the experiments, the Porod slope (p) decreased from ~3.4 to ~2.5. In the pure ACC experiment, p increased subsequently to ~2.9 during stage three, while in the SO$_{4(repl)}$ experiment, p remained ~2.5.

If: $1 < p < 3$, the scattering particles are volume fractals with a mass fractal dimension:

$$D_m = p \qquad \text{(Eq. S1);}^4$$

If: $3 < p < 4$, the scattering particles have fractal surfaces with a surface fractal dimension of:

$$D_s = 6 - p \qquad \text{(Eq. S2).}^5$$

Initially when the only phase was ACC (Figure 2A), p had a value of ~3.4 (Figure S3). This indicates that the ACC particles had rough surfaces, with a surface fractal dimension (D_s) of 2.6 (Eq. S1)[4]. The decrease in p during the first 4 minutes of the experiments coincides with the decrease in α$_{ACC}$ (Figure 2A). When all ACC was transformed to vaterite, p reached its lowest value of ~2.5. This indicates the vaterite spherulites have a

mass fractal character ($D_m \approx 2.5$ (Eq. S2))[5], which has ben shown previously for polycrystalline/porous aggregates.[6] The decrease in p during stage two can be attributed to the transformation of the remnant ACC in suspension to vaterite (Figure 2A and 3B). The increase in p during stage three in the pure ACC system (Figure S3), indicates that the fractal appearance of the vaterite spherulites decreases (i.e. D_m increased from ~2.5 to 2.9 (Eq. S2))[5]. Pipich et al.[6] have determined previously, that this correlates well with an increase in the crystallite size. During stage three in the $SO_{4(repl)}$ system, p remained at ~2.5 (Figure S3).[5] This indicates that the fractal appearance of the vaterite spherulites did not change significantly.

Table S2 Summary of the PHREEQC[7] modeling results. The measured pH, total calcium and total sulfate concentrations were used as input parameters to calculate the total inorganic carbonate (TIC), the aqueous carbonate speciation and the *SI* with respect to vaterite.

Pure ACC		Total concentrations (mM)			Aqueous speciation (mM)				
time (min)	pH	Ca	TIC	SO$_4$	Ca^{2+}	CO_3^{2-}	HCO_3^-	SO_4^{2-}	SI (vaterite)
1	9.5	26	30	0	20	4.0	7.3	0	2.3
2	8.5	11	18	0	9.9	0.71	12	0	1.2
5	8.2	9.2	17	0	8.7	0.36	12	0	0.89
8	8.2	8.9	16	0	8.4	0.35	12	0	0.86
10	8.2	9.0	16	0	8.5	0.35	12	0	0.87
20	8.2	8.7	16	0	8.2	0.34	12	0	0.84
30	8.2	8.5	16	0	8.0	0.32	11	0	0.81
SO$_{4(repl)}$		Total concentrations (mM)			Aqueous speciation (mM)				
time (min)	pH	Ca	TIC	SO$_4$	Ca^{2+}	CO_3^{2-}	HCO_3^-	SO_4^{2-}	SI (vaterite)
1	8.8	75	45	45	57	2.1	22	23	2.5
2	8.1	53	32	36	44	0.48	22	19	1.7
5	8.0	49	28	34	42	0.31	20	18	1.5
8	7.9	48	27	34	41	0.28	19	18	1.5
10	7.9	49	28	34	42	0.28	19	18	1.5
20	7.9	49	26	36	42	0.26	18	19	1.4
30	7.9	50	27	36	42	0.27	19	19	1.4
SO$_{4(add)}$		Total concentrations (mM)			Aqueous speciation (mM)				
time (min)	pH	Ca	TIC	SO$_4$	Ca^{2+}	CO_3^{2-}	HCO_3^-	SO_4^{2-}	SI (vaterite)
1	9.6	32	39	48	22	5.4	8.5	27	2.5
2	8.9	11	35	38	8.5	2.4	19	22	1.7
5	8.7	11	37	38	8.3	1.8	23	22	1.6
8	8.7	11	36	38	8.1	1.7	22	22	1.5
10	8.7	10	35	39	8.1	1.7	22	22	1.5
20	8.6	10	34	39	8.1	1.6	22	23	1.5
30	8.6	10	33	40	8.1	1.5	21	23	1.5

Table S3 The rate constants (k) and induction time (t_0) derived from the $\alpha_{vaterite}$ data fitted with the JMAK model[8-11].

JMAK Equation:	$\alpha(t) = 1 - \exp\left[k(t - t_0)^4\right]$		
Experiment	Variable	Value	Error
Pure ACC	k (min^{-4})	48.7	8.8
Adj. $R^2 = 0.9888$	t_0 (min)	0.93	0.02
SO$_{4(repl)}$	k (min^{-4})	11.7	2.5
Adj. $R^2 = 0.9828$	t_0 (min)	0.98	0.03
SO$_{4(add)}$	k (min^{-4})	9.2	2.3
Adj. $R^2 = 0.9727$	t_0 (min)	1.37	0.03

References

1. Tobler, D. J.; Shaw, S.; Benning, L. G., Quantification of initial steps of nucleation and growth of silica nanoparticles: An in-situ SAXS and DLS study. *Geochimica et Cosmochimica Acta* **2009,** 73, (18), 5377-5393.
2. Benning, L. G.; Waychunas, G. A., Nucleation, Growth, and Aggregation of Mineral Phases: Mechanisms and Kinetic Controls. In *Kinetics of Water-Rock Interactions*, Brantley, S.; Kubicki, J.; White, A., Eds. Springer-Verlag: New-York, 2007; pp 259-333.
3. Schmidt, P. W., Small-Angle Scattering Studies of Disordered, Porous and Fractal Systems. *Journal of Applied Crystallography* **1991,** 24, 414-435.
4. Teixeira, J., Small-Angle Scattering by Fractal Systems. *Journal of Applied Crystallography* **1988,** 21, 781-785.
5. Bale, H. D.; Schmidt, P. W., Small-Angle X-Ray-Scattering Investigation of Submicroscopic Porosity with Fractal Properties. *Physical Review Letters* **1984,** 53, (6), 596.
6. Pipich, V.; Balz, M.; Wolf, S. E.; Tremel, W.; Schwahn, D., Nucleation and Growth of CaCO3 Mediated by the Egg-White Protein Ovalbumin: A Time-Resolved in situ Study Using Small-Angle Neutron Scattering. *Journal of the American Chemical Society* **2008,** 130, (21), 6879-6892.
7. Parkhurst, D. L.; Appelo, C. A. J., *User's guide to PHREEQC (version 2) — a computer program for speciation, batch-reaction, one-dimensional transport, and inverse geochemical calculations*. U.S. Geological Survey Denver, Colorado, 1999; p 312.
8. Avrami, M., Kinetics of phase change, I. General Theory. *Journal of Chemical Physics* **1939,** 7, 1103-1112.
9. Avrami, M., Kinetics of phase change, II. Transformation-Time Relations for Random Distribution of Nuclei. *Journal of Chemical Physics* **1940,** 8, 212-224.
10. Avrami, M., Kinetics of Phase Change, III. Granulation, Phase Change, and Microstructure. *Journal of Chemical Physics* **1941,** 9, 177-184.
11. Johnson, W. A.; Mehl, R. F., Reaction kinetics in processes of nucleation and growth.

Transactions of the American Institute of Mining, Metallurgical and Petroleum Engineers **1939,** 135, 416-442.